Journal of Applied Fluid Mechanics, Vol. 11, No. 3, pp. 779-786, 2018.
Available online at www.jafmonline.net, ISSN 1735-3572, EISSN 1735-3645.
DOI: 10.29252/jafm.11.03.27796

Rollover Mechanism Methodology of LNG Tank with Gas-Liquid Stratification Based on Curvelet Finite Element Method and Large Eddy Simulation Technology

B. Zhao†, S. Han, L. Xu, C. Shi, D. Gao and Y. Zhang

School of Mechanical Engineering, Liaoning Shihua University, Fushun, Liaoning 113001, China

†Corresponding Author E-mail:zbzbz0203288@163.com

(Received March 18, 2017; accepted December 23, 2017)

ABSTRACT

The rollover phenomenon of LNG tank has great threat to secure storage of LNG, therefore the Curvelet finite element method combing the large eddy simulation technology to analyze the rollover mechanism. Firstly, the basic principles of Curvelet transform are studied, the mathematical model and properties of Curvelet transform have been discussed. Secondly, theoretical models of rollover of LNG tank with gas-liquid stratification based on large eddy simulation are put forward, and then rollover Curvelet finite element of LNG tank with gas and liquid phase stratification is established. Finally, the rollover mechanism analysis of LNG tank with gas and liquid stratification is carried out based on different simulation method. The changing rules of mean velocity of interface between gas and liquid phase LNG gas phase and liquid phase LNG is obtained, and the changing rules mean velocities of gas and liquid phase LNG for different heat flux density are also obtained. Comparing results show that the Curvelet finite element method has higher computing precision than traditional finite element method.

Key words: Rollover mechanism; LNG tank; Curvelet finite element; Large eddy simulation.

1. INTRODUCTION

With the adjustment of national energy structure and improvement of environmental requirements, the liquid natural gas (LNG), as a kind of clean energy without color, taste, toxic and corrosion, has been applied widely in China. LNG tank is a main storage device of LNG. LNG in tank will generate the static evaporation due to interference arising from outer heat source, the LNG vaporizes on heating, and then pressure in tank rises accordingly. The component with low boiling point in upper liquid evaporates preferentially, and then two or more LNG stratification with different density and temperature form. When the density and temperature differences reach to a certain value, and the rollover will be caused, and rapid evaporation will be formed. In addition, the heat leakage of tank wall and heat and mass exchange between different layer make two layers mix rapidly to occur rollover phenomenon. The bottom layer liquid has big density and high temperature, and the liquid is in overheating state. The lower liquid rolls to upper layer, a large amount of liquid vaporizes in a short period of time owing to the change of pressure. The rapidly changing pressure make safety valve move frequently, and a amount of LNG is lost due to emission out of control. The explosive mixed cloud cluster will form in the surrounding space, or the boiling liquid expanding vapour explosion can be raised. The rollover of LNG tank has great threat to secure storage of LNG, therefore it is necessary to take certain precautions to avoid the occurrence of rollover phenomenon in LNG transport and storage. Since the rise of LNG industry in 1970s, many LNG rollover accidents have already happened.

In recent years, the rollover phenomenon of tank has been concerned by many scientists, and some excellent achievements have been obtained. Osama A.Marzouk and Ali H.Nayfeh (2009) studied the performance of passive and active anti-roll tank (ART) system, each ART consists of three identical tanks, distributed along the center line of the ship. The loads exerted on the ship by the ARTs could reduce the excessive roll motions. Christian Holden *et al*. (2011) propose two new models of u-shaped anti-roll tanks for ships and a simplified nonlinear model. The models were derived by Lagranian

mechanics. Results showed that the proposed nonlinear models were valid for large roll amplitudes. Even at moderate roll angles, the nonlinear models had three orders of magnitude lower mean square error relative to experimental data than the linear models. AmirKolaei *et al* (2014) proposed a model of a partly-filled tank of arbitrary cross section for predicting transient lateral slosh force and overturning moment by linear slosh theory. Results suggested that a tank cross-section with lower overall center of mass and lower critical slosh length yielded an enhanced roll stability limit under medium- and high-fill conditions. Wenhua Zhao and Finlay McPhail (2017) carried out the experimental study for a barge-like vessel carrying two spherical tanks. These tanks were filled with water to different volumes to simulate different loads. Results showed that roll response of the vessel with liquid cargo inside spherical tanks was greater than observed for the equivalent 'frozen-cargo' case. Yuxing Li *et al*. (2015) studied the rollover phenomenon in LNG storage based on experiment and FLUENT software. Experimental results showed that initial phase where rollover occurred near the side wall of the storage tank, and the turbulent phase where rollover transferred to the center of the tank. Simulation results showed that rollover coefficient initially increases within a small scope and then increased rapidly with the increment of initial density difference. Mohammad RezaAssari *et al*. (2018) studied the thermal stratification of water storage tank on solar collector performance based on experiment. Three experiments with different conditions were carried out, and results showed that lowering the temperature of the lower layers in the tank would enhance the solar collector performance, and the tank bottom temperature and the collector efficiency were inversely related. As seen from existing achievements, the researches mainly focused on liquid-liquid stratification and rollover of tank, and performance of anti-roll tanks in ship. The gas-liquid phase stratification of LNG tank has not been reported so far. Therefore the rollover mechanism of LNG tank with gas-liquid phase stratification should be studied in depth.

Rollover of LNG tank with gas-liquid stratification belongs to nonlinear problem, therefore an effective numerical method should be chosen to enhance the computing precision and efficiency of simulation analysis. Wavelet finite element method is an effective tool for analyzing the nonlinear problems. In recent years, the wavelet finite element method has been applied to analyze the nonlinear problem, and some excellent achievements have been obtained. Bin Zhao *et al*. (2016) studied the heat transfer of single screw compressor based on fuzzy random wavelet finite element method. The heat transfer wavelet finite element model of single screw compressor was constructed using Hermitian wavelet function, and the fuzzy random Hermitian wavelet finite element model was established based on λ level set theory. Mojtaba Aslami and Pavel A.Akimov. (2016) proposed an efficient multilevel based on coupling of finite element method and discrete wavelet transform, which was applied in local static analysis of plates. The problem was discretized using finite elements and the governing equation was transformed into a localized one by using the discrete Haar wavelet. Simulation results showed that the new method could offer more accurate results for the selected regions comparing with the finite element solutions, and the efficiency of the new method was considerable improved. Yan Azdoud *et al*. (2017) extended a wavelet enrichment adapted finite element model for elastic materials to finite deformation, crystal plasticity analysis of polycrystalline micro-structures. The new model created an optimal set of scaling and multi-resolution wavelet basis functions, and the convergence rates and computational efficiency were verified based on validation tests. Ali Mokhtari *et al*. (2017) formulated the wavelet-based spectral finite element model for time and wave domain dynamic analysis of an axially moving Timoshenko beam subjected to axial pretension. The localized nature of Daubechies wavelet basis functions were used for temporal discretization of the governing partial differential equations into a set of ordinary differential equations. The high precision of new method was evaluated by comparing analysis. As seen from the current researching achievements, the wavelet finite element has been applied in many fields. Application results showed that the wavelet finite element can solve nonlinear problems effectively, therefore applying the wavelet finite element method in analyzing the rollover problem of LNG tank is feasible. The Curvelet tansform has characteristics of multi-scale and multi-direction, which can carry out better sparse representation for edge curve than wavelet transform. It has characteristics of anisotropy and completeness, which has better approximation ability than wavelet transform. Therefore Curvelet transform is used to introduce into the traditional finite element method to generate the Curvelet finite element method. In addition, the rollover process of LNG tank with gas and liquid phase stratification has strong turbulence characteristics, therefore the large eddy simulation method is applied in this research to enhance correctness of rollover analysis of LNG tank.

1 BASIC PRINCIPLE OF CURVELET TRANSFORM

In given feature point set R^2, x is the location parameter of space, ω is the variable of the frequency domain, r and θ are the polar coordination under frequency domain.

Let us assume that "radius window" $W(r)$ and "angle window" $V(r)$ are smooth, non-negative and real valued, $V(t)$ satisfies the following conditions:

$$\sum_{j=-\infty}^{\infty} W^2(2^j r) = 1, \ r \in (0.75, 1.5) \tag{1}$$

$$\sum_{j=-\infty}^{\infty} V^2(r - l) = 1, \ r \in (-0.5, 0.5) \tag{2}$$

The "wedged" window under polar coordination U_j is formulated by:

$$U_j(r,\theta) = 2^{-3j/4} W(2^{-j} r) V(\frac{2^{[j/2]}\theta}{2\pi}) \tag{3}$$

Where [*j*/2] is the integer part of *j*/2.

The rotation angle sequence with the same interval and displacement parameter is expressed by

$$\theta_l = 2\pi \times 2^{-[j/2]} \times l, l = 0,1,2,...,$$

$$0 \le \theta_l \le 2\pi \tag{4}$$

$$k = (k_1, k_2) \in Z^2 \tag{5}$$

The Curvelet transform under scale 2^{-j}, directional angle θ_l, and location $x_k^{(j,l)} = R_{\theta_l}^{-1}(k_1 \times 2^{-j}, k_2 \times 2^{-j/2})$ is formulated by (Nayak *et al*., 2017):

$$\phi_{j,k,l}(x) = \phi_l(R_{\theta_l}(x - x_k^{(j,l)})) \tag{6}$$

Where R_θ is the rotation using θ as radian.

The local window under Cartesian coordinate system is listed as follows:

$$\overline{U}_j(\omega) = \tilde{W}_j(\omega) V_j(\omega) \tag{7}$$

Where $\tilde{W}_j(\omega) = \sqrt{\Theta_{j+1}^2(\omega) - \Theta_j^2(\omega)}$,

$V_j(\omega) = V(2^{[j/2]} \frac{\omega_2}{\omega_1})$, Θ is the inner product of the one-dimensional low-pass window, which is formulated by:

$$\Theta_j(\omega_1, \omega_2) = \Theta(2^{-j}\omega_1)\Theta(2^{-j}\omega_2) \tag{8}$$

The slope with the same interval can be described by expression $\tan\theta_l = l \times 2^{-[j/2]}$, $l = -2^{[j/2]}, \cdots, 2^{[j/2]} - 1$, and then the expression (8) can be transferred to the following formulation:

$$\overline{U}_{j,l(\omega)} := W_j(\omega) V(S_{\theta_l}\omega) \tag{9}$$

Where $S_\theta = \begin{bmatrix} 1 & 0 \\ -\tan\theta & 1 \end{bmatrix}$, and then the Cartesian Curvelet can be expressed by (Dong *et al*., 2017):

$$\tilde{\varphi}_{j,l,k}(k) = 2^{3j/4} \tilde{\varphi}_j(S_{\theta_l}^T (x - S_{\theta_l}^{-T} b)) \tag{10}$$

where b takes the discrete value $(k_1 \times 2^{-j}, k_2 \times 2^{-j/2})$. .

2 THEORETICAL MODELS OF ROLLOVER OF LNG TANK WITH GAS-LIQUID STRATIFICATION BASED ON LARGE EDDY SIMULATION

Rollover is the main reason that causes the instability accident of LNG storage and transportation. The rollover is the process of intense evaporation, which can lead to the rapid pressure rise of LNG tank. If the protective measures are improper, the serious accident will happen.

The thermal stratification of LNG in storage tank can be generated because of all kinds of reasons. The LNG tank concludes gas and liquid phase region, and the liquid phase region concludes stratification and main flow area. The LNG with big density is at the bottom of the liquid phase region, and the natural convection of upper and lower layers is limited to each layer.

Because the rollover process of LNG tank with gas and liquid phase stratification belongs to turbulence, the large eddy simulation method is applied to analyze the rollover of LNG tank to improve calculating precision of numerical analysis. The pulsation with small scale in turbulence is eliminated by using filtering method, and the filtering process is completed based on integral operation, the corresponding formulation is expressed by

$$\overline{u}_i(x,t) = \int_V u_i(\xi,t) G(x-\xi) dV \tag{11}$$

Where $G(x-\xi)$ is the filtering function, and the cartridge filtering function is used in this research, which is expressed as follows:

$$G(x-\xi) = \begin{cases} \frac{1}{\Delta}, |\eta| \le \frac{\Delta}{2} \\ 0, |\eta| > \frac{\Delta}{2} \end{cases} \tag{12}$$

Where Δ is the grid average scale, η is the dissipation scale, ξ is the initial horizontal coordinate.

The controlling equation of large eddy simulation can be obtained through filtering process, which is expressed as follows (William *et al*., 2017):

$$\frac{\partial \overline{u}_i}{\partial t} + \frac{\partial \overline{u}_i \overline{u}_j}{\partial x_j} = -\frac{1}{\rho}\frac{\partial \overline{p}}{\partial x_i} - \frac{\partial \tau_{ij}}{\partial x_j} + \mu \frac{\partial^2 \overline{u}_i}{\partial x_j \partial x_j} \tag{13}$$

$$\frac{\partial \overline{u}_i}{\partial x_i} = 0 \tag{14}$$

Where ρ is the density of gas and liquid phase LNG, μ is the kinematic viscosity of gas and liquid phase LNG, τ_{ij} is the sub grid stress. And the corresponding expression can be confirmed based on strain rate of large scale flow field, which is expressed as follows:

$$\tau_{ij} - \frac{1}{3}\tau_{kk}\delta_{ij} = -2\mu_t \overline{S}_{ij} \tag{15}$$

$$\overline{S}_{ij} = \frac{1}{2}(\frac{\partial \overline{u}_i}{\partial x_j} + \frac{\partial \overline{u}_j}{\partial x_i}) \tag{16}$$

Where δ_{ij} denotes the Kronecker mark, $\overline{S}_{ij}$ denotes the large scale deformation rate tensor, μ_t denotes the eddy viscosity coefficient of sub grid, which is calculated based on Smagorinsky model, and the corresponding expression is listed as follows:

$$\mu_t = (C_s\overline{\Delta})^2\left|\overline{S}\right| \tag{17}$$

Where $\left|\overline{S}\right| = \sqrt{2\overline{S}_{ij}\overline{S}_{ij}}$, C_s denotes the empirical Smagorinsky coefficient, $C_s = 0.2$ in this research.

The state equation of mass density is expressed as follows (Volpiani *et al*., 2017):

$$\rho = \rho_0\left[1-\alpha(T-T_0)\right] \tag{18}$$

Where α denotes the thermal expansion coefficient, ρ_0 .and T_0 are the initial density and temperature respectively.

For qth phase of the multiphase flow, the volume ratio equation is expressed as follows:

$$\frac{\partial(\alpha_q\rho_q)}{\partial t} + \nabla.(\alpha_q\rho_q\overline{u}_q) = \sum_{p=1}^{n}\dot{m}_{pq} \tag{19}$$

Where α_q denotes the volume fraction of qth phase, ρ_q denotes the density of qth phase, $\overline{u}_q$ denotes the velocity of qth phase, $\dot{m}_{pq}$ denotes the mass transfer from pth phase to qth phase.

3. ROLLOVER CURVELET FINITE ELEMENT OF LNG TANK WITH GAS AND LIQUID PHASE STRATIFICATION

The Curvelet functions $\tilde{\varphi}^1_{j,l,k}(\alpha)$ and $\tilde{\varphi}^2_{j,l,k}(\beta)$ can generate multi-resolution subspaces $\left\{V_j^1\right\}$ an $\left\{V_j^2\right\}$, the tensor product of subspaces form the higher order space, which is expressed as follows:

$$V_j = V_j^1 \otimes V_j^2 \tag{20}$$

Where V_j denotes the tensor space, $j = 0,1,\cdots,N-1$; $\otimes$ denotes tensor product operator, α and β denote the local coordinates.

The Curvelet function in sub space is expressed as follows:

$$\vec{\phi}^1_{j,l,k} = \left\{\tilde{\phi}^1_{j,l,k}(\alpha), \tilde{\phi}^1_{j,l,k}(\alpha+1), \cdots, \tilde{\phi}^1_{j,l,k}(\alpha+(N-2))\right\} \tag{21}$$

$$\vec{\phi}^2_{j,l,k} = \left\{\tilde{\phi}^2_{j,l,k}(\beta), \tilde{\phi}^2_{j,l,k}(\beta+1), \cdots, \tilde{\phi}^2_{j,l,k}(\beta+(N-2))\right\} \tag{22}$$

The Curvelet function on higher order space $\left\{V_j\right\}$ is expressed as follows:

$$\vec{\phi}_{j,l,k} = \vec{\phi}^1_{j,l,k} \otimes \vec{\phi}^2_{j,l,k} \tag{23}$$

The Curvelet function is used as the interpolating function to establish the Curvelet finite element, and the temperature function $\overline{u}_i(\alpha,\beta)$ can be expressed as follows (Kumar and Rai, 2016):

$$\overline{u}_i(\alpha,\beta) = \vec{\phi}.\vec{c}_w \tag{24}$$

where $\vec{\phi}$ is Curvelet function, $\vec{c}_w$ denotes wavelet coefficient vector, $\vec{c}_w = \left(c_{w,0}, c_{w,1}, \cdots, c_{w,-(N-2)}\right)$, $c_{w,0}, c_{w,1}, \cdots, c_{w,-(N-2)}$ $a_0, \cdots, a_{-(N-2)}$ are elements of $\vec{c}_w$, and the relationships between the local and global coordinates can be expressed as follows:

$$a = \frac{x-x_1}{x_2-x_1} \tag{25}$$

$$\beta = \frac{y-y_1}{y_2-y_1} \tag{26}$$

Where x_1 and x_2 are the maximum and minimum values of x coordinate for Curvelet finite element; y_1 and y_2 are the maximum and minimum values of y coordinate.

Equivalent integral form of two-dimensional turbulent flow is expressed as follows:

$$\int_{S_e}\left[\begin{array}{l}\delta\overline{u}_i\left(\frac{\partial\overline{u}_i}{\partial t}\right) + \frac{\partial\left(\delta\overline{u}_i\right)}{\partial x_j}\left(\frac{\partial\overline{u}_j}{\partial x_j}\right) \\ + \frac{\partial\left(\delta\overline{u}_j\right)}{\partial x_j}\left(\frac{\partial\overline{u}_i}{\partial x_j}\right) - \mu\frac{\partial^2\left(\delta\overline{u}_j\right)}{\partial x_i\partial x_j}\end{array}\right]d\alpha d\beta$$
$$+\frac{1}{\rho}\int_{\Gamma_0}\delta(\overline{u}_i)\left(\frac{\partial\overline{p}}{\partial x_i} + \frac{\partial\tau_{ij}}{\partial x_j}\right)dl = 0 \tag{27}$$

Where e denotes the Curvelet finite element, S denotes the volume of Curvelet finite element, l denotes the linear boundary of Curvelet finite element.

Putting formula (24) into formula (27) considering the arbitrariness of $\delta\overline{u}_i$, the Curvelet finite element equation is expressed as follows:

$$A\frac{\partial\overline{u}_i}{\partial t} + B\overline{u}_i = F \tag{28}$$

Where A denotes the fluid mass matrix, B denotes fluid stiffness matrix, F denotes the node load vector of fluid element.

$$A_{ij} = \sum_e A^e_{G_i} + \sum_e A^e_{L_i} \tag{29}$$

$$B_{ij} = \sum_e B^e_{ij} \tag{30}$$

$$F_{ij} = \sum_e F_{G_i}^e + \sum_e F_{L_i}^e \tag{31}$$

where $A_{G_i}^e$ denotes the contribution of gas phase fluid element on mass matrix, $A_{L_i}^e$ denotes the correction of liquid phase fluid element on mass matrix, B_{ij}^e denotes the contribution of element on fluid stiffness matrix, $F_{Q_i}^e$ is the node load generated by gas phase fluid element, $F_{L_i}^e$ is the node load formed by the liquid phase fluid element. The matrix elements are expressed as follows:

$$A_{G_i}^e = \int_{S_e} \left(\frac{\partial \Phi_i}{\partial \alpha} \cdot \frac{\partial \Phi_j}{\partial \alpha} + \frac{\partial \Phi_i}{\partial \beta} \cdot \frac{\partial \Phi_j}{\partial \beta} \right) d\alpha d\beta \tag{32}$$

$$A_{L_i}^e = \int_{S_e} \left(\frac{\partial^2 \Phi_i}{\partial \alpha \partial \beta} \right) d\alpha d\beta \tag{33}$$

$$B_{ij}^e = \int_{S_e} \left(\frac{\partial \Phi_i}{\partial \alpha} + \frac{\partial \Phi_j}{\partial \beta} \right) d\alpha d\beta \tag{34}$$

$$F_{G_i}^e = \int_{\Gamma_e} \frac{\partial \overline{p}}{\partial \alpha} \Phi_i dl \tag{35}$$

$$F_{L_i}^e = \int_{\Gamma_e} \frac{\partial \tau_{ij}}{\partial \alpha} \Phi_i dl \tag{36}$$

where Φ_i and Φ_j denote the weighted functions.

The recurrent formula is used to solve the formula (14), which is expressed as follows:

$$\overline{B}\overline{u}_{i,n+1} = \overline{R}_{n+1} \tag{37}$$

where $\overline{B} = \frac{A}{\Delta t} + \eta B$,

$\overline{R}_{n+1} = \left[A / \Delta t - (1-\eta) B \right] u_{i,n} + (1-\eta) F_n + \eta F_{n+1}$,

η denotes the interpolation coefficient, Δt denotes the time step.

The corresponding algorithm procedure is constructed, which is listed as follows:

Step 1: Coefficient matrices A and B are obtained based on formulas (32)-(34);

Step 2: The initial fluid velocity is set as $u_{i,0}$;

Step 3: The values of η and Δt are confirmed according to real situation of problems.

Step 4: The effective coefficient matrix is generated by the following expression $\overline{B} = \frac{A}{\Delta t} + \eta B$.

Step 5: The triangular decomposition is carried out for $\overline{B}$ based on the following expression:

$$\overline{B} = LDL' \tag{38}$$

Where L is the low triangle matrix, D is the diagonal matrix with positive element.

Step 6: The initial vector R_{n+1} is chosen.

Step 7: The effective vector F_{n+1} is generated based on formula (39).

Step 8: The $u_{i,n+1}$ can be solved through the following expression:

$$LDL'\overline{u}_{i,n+1} = \overline{F}_{n+1} \tag{39}$$

Step 8: The calculating results is judged whether meets the error condition predefined, if it meets the error condition, the algorithm is over; otherwise if it does not meet the error condition, return to step 6.

4. ROLLOVER MECHANISM ANALYSIS OF LNG TANK WITH GAS AND LIQUID STRATIFICATION

The physical model of thermal stratification and rollover of LNG tank can be simplified as follows: the capacity of LNG tank is 10000m3, the diameter of LNG tank is 20m, and the LNG tank uses 2D model, and the thickness of LNG tank is ignored. Two layers with same height in the total LNG tank are used as researching objects, and the top layer is gas phase LNG, the bottom layer is liquid phase LNG, and the interface is fixed. The simplified physical model of LNG tank is shown in Fig. 1.

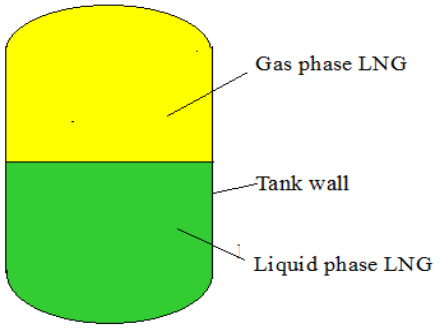

Fig. 1. Simplified physical model of LNG tank.

In order to verify the reliability of the Curvelet finite element method, the mean velocity of interface between gas and liquid phase LNG are obtained based on traditional finite element method, Curvelet finite element method and test respectively.

The gas phase LNG is meshed by 420 Curvelet finite elements and 2480 traditional finite elements, and the liquid phase LNG is meshed by 352 Curvelet finite elements and 2268 traditional finite elements. The mean velocity of LNG is measured by fluid velometer. The mean velocity of interface between gas and liquid phase LNG gas phase and liquid phase LNG are shown in Fig. 2.

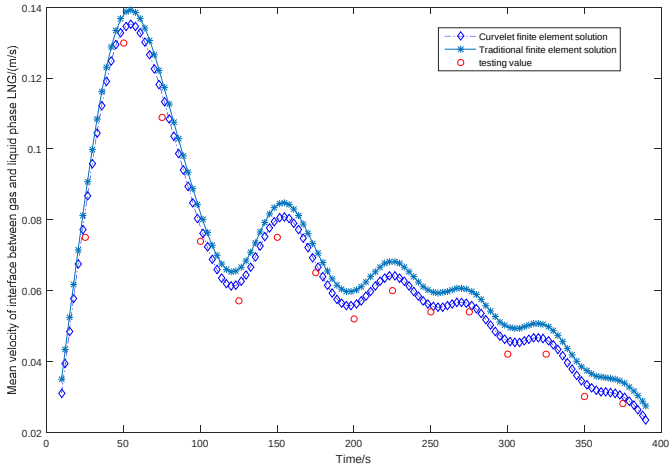

Fig. 2. Mean velocity of interface between gas and liquid phase LNG gas phase and liquid phase LNG.

As seen from Fig. 2, the velocity of interface between gas and liquid phase LNG increases rapidly in 0-60s, and it reaches maximum velocity at 50s, because the density of interface between gas and liquid phase LNG changes quickly. The interface between gas and liquid phase LNG produces huge fluctuations under the effect of compression between gas and liquid phase LNG, and then the rollover of LNG tank happens. The velocity of interface between gas and liquid phase LNG decreases in 60-120s, this is due to reduction of density caused by fierce action between gas and liquid phase LNG in early stage, and then the degree of compression between gas and liquid phase reduces accordingly. The rollover phenomenon still exists after 120s, however the compression dynamic decreases continuously, and then the severe degree of rollover reduces. The main reason is decreasing of density, and the velocity of interface between gas and liquid phase LNG decreases remains stable gradually.

In addition, although the number of the Curvelet finite elements used to mesh the LNG tank is less than that of the traditional finite elements, the Curvelet finite element solution is closer to the testing value than traditional finite element solution, therefore the Curvelet finite element method has higher computing precision.

The rollover has many affecting factors, the effect of environmental heat leakage on it is studied firstly. The mean velocities of gas phase and liquid phase LNG are calculated when the heat flux densities are 35W/m^2 and 55W/m^2 respectively, and results are shown in Figs. 3 and 4 respectively.

As seen from Figs 3 and 4, the maximum mean velocity of gas and liquid phase LNG increases when the heat flux density increases. With increasing of environmental heat leakage, the gas and liquid phase LNG flow rapidly, and then the mean velocities of gas and liquid phase LNG increase accordingly. The accumulated heat of gas and liquid phase LNG increases with increasing of environmental heat leakage, and then the rollover of LNG tank is becoming increasingly intense. When the heat flux density increases from 35W/m^2 to 55W/m^2, the increased range of mean velocity of liquid phase LNG is bigger than that of gas phase LNG. In addition, the maximum mean velocity of gas phase LNG is bigger than that of interface between gas and liquid phase LNG, and the maximum mean velocity of liquid phase is less than that of interface between gas and liquid phase LNG. The comparing results between the Curvelet finite element solutions and traditional finite element solutions also show that the Curvelet finite element method has better computing reliability than traditional finite element method.

5. CONCLUSIONS

Storage and transportation safety of LNG is important in High speed development period, therefore it is necessary to study the rollover mechanism of LNG tank. The rollover model of LNG tank is constructed based on large eddy simulation technology. The Curvelet finite element model is established through combing the Curvelet transform and traditional finite element method to solve the rollover model of LNG model. The rollover procession of LNG tank can be analyzed effectively. Simulation results show that velocity of interface between gas and liquid phase LNG increases rapidly in 0-60s, and then tends to be stable later. The Curvelet finite element can obtain higher computing precision than traditional finite

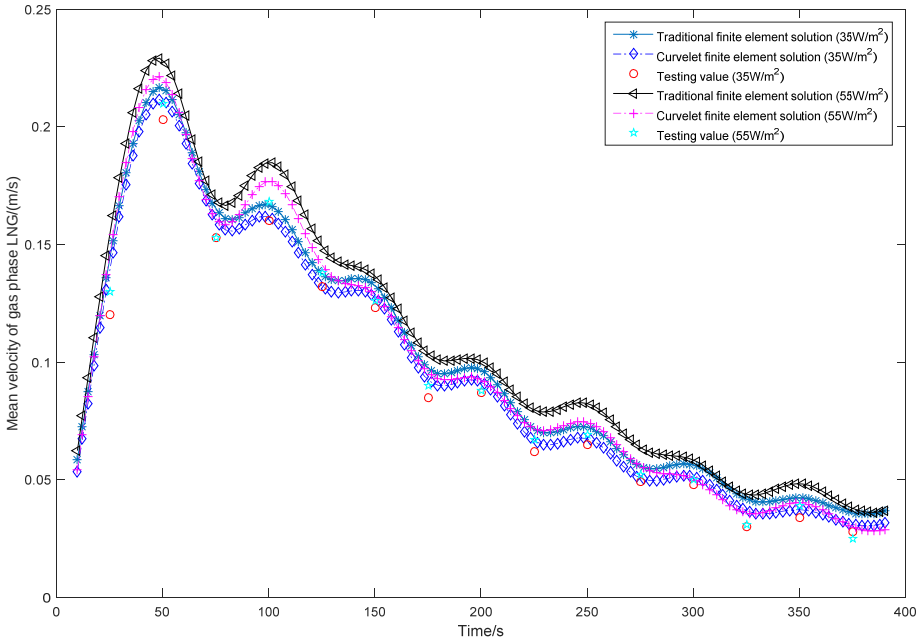

Fig. 3. Mean velocity of gas phase LNG for different heat flux density.

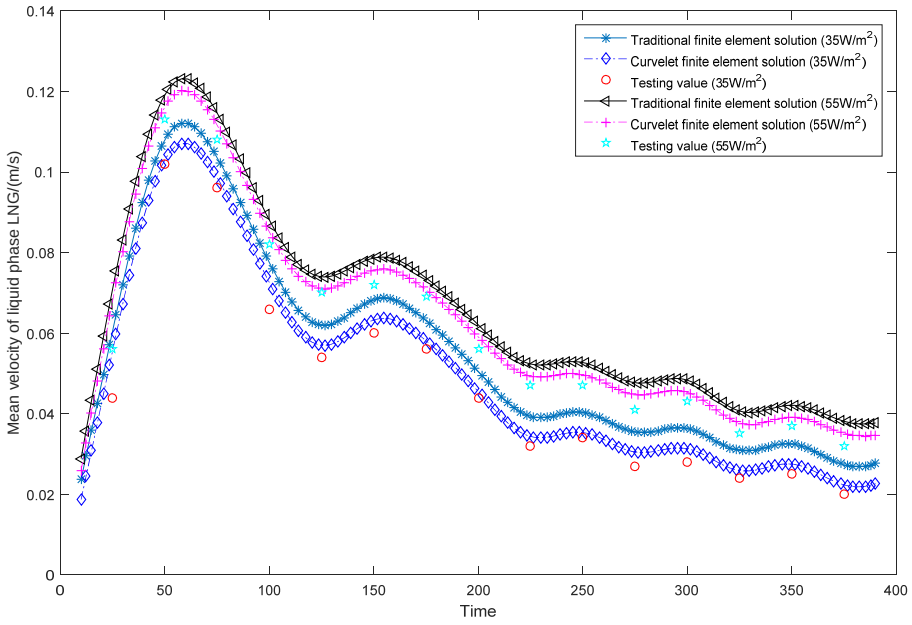

Fig. 4. Mean velocity of liquid phase LNG for different heat flux density.

element method using less elements. The effect of environmental heat leakage on rollover of LNG tank is also studied, and the rollover degree of LNG tank increases in intensity with increasing of heat flux density. The influence of other affecting factors on rollover of LNG tank can be analyzed in depth by using the Curvelet finite element method, and the better computing precision can be obtained. The theoretical analysis results can offer beneficial guidance for taking effective measures to prevent rollover of LNG tank.

ACKNOWLEDGEMENTS

This research was supported by the national natural science foundation (51206075).

REFERENCES

Amir, K., R. Subhash and J. R. Marc (2014). Effects of tank cross-section on dynamic fluid slosh loads and roll stability of a partly-filled tank truck, *European Journal of Mechanics-B/Fluids, 46*(2), 46-58.

Aslami, M. and P. A. Akimov (2016). Wavelet-based finite element method for multilevel local plate analysis, *Thin-Walled Structures, 98*(1), 392-402.

Azdoud, Y., J. H. Cheng and S. Ghosh (2017). Wavelet-enriched adaptive crystal plasticity finite element model for polycrystalline microstructures, *Computer Methods in Applied Mechanics and Engineering, 327*(12), 36-57.

Christian, H., P. Tristan and I. F. Thor (2011). A Lagrangian approach to nonlinear modeling of anti-roll tanks, *Ocean Engineering, 38*(2–3), 341-359.

Dong L. Q., D. Y. Wang, Y. M. Zhang and D. T. Zhou (2017). Signal enhancement based on complex curvelet transform and complementary ensemble empirical mode decomposition, *Journal of Applied Geophysics, 144*(9), 144-150.

Kumar, D. and K. N. Rai (2016). A study on thermal damage during hyperthermia treatment based on DPL model for multilayer tissues using finite element Legendre wavelet Galerkin approach, *Journal of Thermal Biology, 62*(12), Part B, December 2016, 170-180

Li, Y. X., Z. L. Li and W. C. Wang (2015). Simulating on rollover phenomenon in LNG storage tanks and determination of the rollover threshold, *Journal of Loss Prevention in the Process Industries, 37*(9), 132-142.

Mohammad, R. A., B. T. Hassan and J. M. Mohammad (2018). Experimental study on destruction of thermal stratification tank in solar collector performance, *Journal of Energy Storage, 15*(2), 124-132.

Mokhtari, A., H. R. Mirdamadi, M. Ghayour (2017). Wavelet-based spectral finite element dynamic analysis for an axially moving Timoshenko beam, *Mechanical Systems and Signal Processing, 92*(8), 124-145.

Nayak, D. R., R. Dash, B. Majhi and V. Prasad (2017). Automated pathological brain detection system: A fast discrete curvelet transform and probabilistic neural network based approach, *Expert Systems with Applications, 88*(12), 152-164.

Osama, A. M. and A. H. Nayfeh (2009). Control of ship roll using passive and active anti-roll tanks, *Ocean Engineering, 36*(9-10), 661-671.

Volpiani, P. S., T. Schmitt, O. Vermorel, P. Quillatre, D. Veynante (2017). Large eddy simulation of explosion deflagrating flames using a dynamic wrinkling formulationl, *Combustion and Flame, 186*(12), 17-31.

William, P. J., A. J. Marquis and D. Noh (2017). An investigation of a turbulent spray flame using Large Eddy Simulation with a stochastic breakup model, *Combustion and Flame, 186*(12), 277-298.

Zhao, B., M. S. Yang, X. F. Yang, L. Z. Xu, D. K. Gao and Y. Y. Zhang (2016). Heat transfer analysis of single screw compressor under oil atomization based on fuzzy random wavelet finite element method, *International Communications in Heat and Mass Transfer, 77*(10), 43-48.

Zhao, W. H. and F. McPhail (2017). Roll response of an LNG carrier considering the liquid cargo flow, *Ocean Engineering, 129*(1), 83-91.